Environment Protection Engineering

Vol. 43 2017 No. 3

DOI: 10.5277/epe170306

JIAPENG HU[1, 2], DAISHE WU[1], RUIYE RAO[2], RUILAI LIU[2], WENLIANG LAI[3]

ADSORPTION KINETICS OF FLUORIDE ON BONE CHAR AND ITS REGENERATION

The adsorbent of bone char (BC), produced from the pyrolysis of crushed animal bones, was dominated by the mesopores of the Brunauer–Emmett–Teller (BET) surface area. The optimal condition for defluoridation with BC was a pH level near 5.0. Chloride and nitrate ions could increase fluoride adsorption capacity in contrast with the effect of sulfate and carbonate ions. The interchangeability between fluoride and hydroxyl groups on BC sorbent was proved by the Fourier transform infrared spectroscopy. Langmuir equation had a better correlation coefficient than the Freundlich equation at various temperatures. Thermodynamic parameters such as $\Delta G°$, $\Delta H°$, $\Delta S°$, E_a and S^*, have been calculated to describe the nature of fluoride adsorption onto BC. Negative $\Delta G°$ and $\Delta H°$ values at various temperatures indicate a spontaneous process, and its exothermic effect, respectively. However, a positive $\Delta S°$ value represents an increasing process for entropy. The E_a and S^* values ranging from 5 to 40 kJ·mol^{-1} and 0 to 1, respectively, demonstrated that the adsorption is dominated by physical process, although the adsorption kinetic process was involved external diffusion, intraparticle diffusion and chemical reaction equilibrium stage. A high concentration of NaOH solution increases efficiency of removing adsorbed F^- ions from the BC surface.

1. INTRODUCTION

Fluoride is an essential element for human health. The level of fluoride in drinking water is among the important factors in evaluating drinking water quality for human consumption [1]. An abnormal fluoride level, distributed in the natural environment could cause the toxicity or deficiency induced diseases in living organisms [2, 3]. World Health Organization (WHO) recommends that the maximum permissible fluoride level

[1]School of Resources Environmental and Chemical Engineering, NanChang University, Jiangxi Nanchang, 330031, China.

[2]College of Ecology and Resource Engineering, WuYi University, Fujian Wuyishan, 354300, China.

[3]Graduate Institute of Environmental Management, Tajen University, Pingtung, Taiwan, corresponding author W. Lai, e-mail address: lai@tajen.edu.tw

in drinking water should not exceed 1.5 mg·dm^{-3}. The regulation of the Chinese government allows 1.0 mg·dm^{-3} in drinking water [4]. However, the ingestion of elevated concentrations of fluoride can result in fluorosis, which is currently recognized one of the most serious endemics in some regions of the world, especially in China, India, Africa and Mexico, owing to the excess fluoride concentration due to natural occurrence or from industrial activities [5]. In China, reports had proved that 41.76 million people were affected by fluorosis in 1325 different counties, revealing that more than 58.2% of China's population was chronically exposed to high levels of fluoride from drinking water [6].

Several available methods have been applied to remove the excessive fluoride from water body, including precipitation/coagulation, adsorption, ion exchange, reverse osmosis, and electrodialysis [7]. Considering the advantages and disadvantages of these methods, the adsorption process is popularly considered because of its cost-effectiveness, convenience, easy operation, simple design and environmental considerations [8]. In recent years, many efforts have been devoted to investigate and develop new fluoride adsorbents using synthetic, naturally occurring and waste materials from various sources such as activated alumina, tricalcium phosphate, zeolites, and bentonite [9]. Some other low-cost materials have been investigated. Recently, the poorly crystallized apatite such as bone char (BC) apatite, might represent a low-cost adsorbent with a readily available phosphate source [10].

Every year in many countries, many domestic animals are slaughtered for daily meat consumption, resulting in large amounts of bone waste which can be possibly used as feedstock or a fuel for energy generation. Some countries have large hydrocarbon resources being used as an alternative fuel source that bone disposal has a worse impact on sustainable environment. Therefore, the transformation of amassed wastes into BC and other products is an alternative choice in the innovative thinking of cradle to cradle.

BC is a compound of mixed adsorbent comprising carbon distributed throughout the porous structure of hydroxyapatite ($Ca_{10}(PO_4)_6(OH)_2$ or CaHAP). The substitution of BC consists of 76% of CaHAP, indicating not only a major inorganic constituent of teeth and bones but also phosphate rock [11]. The physical and chemical properties of CaHAP have been widely reported, and the anion removal mechanisms have been discussed in terms of their adsorption effect and ion exchange reaction while the ions in solution reacted with the calcium ions in the apatites [12]. Although charred bone was proposed as a medium for water defluoridation more than seven decades ago [13], it is currently one of the most promising defluoridation agents in developing countries. Adsorption of fluoride on BC has been studied in previous works, proving that fluoride can be effectively removed from water solutions [14]. However, the mechanism of fluoride adsorption onto bone char has not been completely elucidated.

In this study, BC was characterized by pH at the point of zero charge (pH_{pzc}), its surface area, and the results of the X-ray diffraction analysis (XRD), scanning electron microscopy (SEM), and Fourier transform infrared spectroscopy (FTIR) for surface and

textural properties. The fluoride adsorption properties of BC were studied through adsorption and desorption experiments. Adsorption isotherms, kinetic and thermodynamic parameters were estimated from experimental results. The fluoride adsorption properties of BC were studied through adsorption and desorption experiments. Adsorption isotherms kinetic and thermodynamic parameters were estimated from experimental results. Thereafter, a mass transfer model was developed to describe the adsorption behavior. The interactions between the BC surface and the fluoride ions in solution were also investigated in order to further understand the adsorption and desorption of fluoride on BC. Finally, the fluoride-saturated BC material was reactivated in a brief example of an industrial application.

2. MATERIALS AND METHODS

Materials. NaOH, $NaNO_3$, Na_2SO_4, Na_3PO_4, Na_2CO_3, HCl and NaF were purchased from Sinopharm Chemical Regent Co., Ltd. (China). Fluoride stock solution of 100 $mg \cdot dm^{-3}$ was prepared from 0.2210 g of NaF dissolved into 1 dm^3 of deionized water produced from a Milli-Q water system (Direct-Q, Millipore Co., Ltd., USA) and then diluted into various concentrations. The granular BC used in this research was manufactured by TianJin QiYuan Hi-Tech Development Center. The BC was washed several times with deionized water and dried in an oven at 105 °C for 24 h. Finally, the dried product was ground into fine powder, and sifted through 74μm sieve. The buffer solution was prepared by the dissolution of 58 g of sodium chloride, 57 cm^3 of acetic acid, 58.8 g of sodium citrate, and 30 g of sodium hydroxide into 1 dm^3 of deionized water with pH range of 5–6. The fluoride concentration in aqueous solution was measured by a fluoride-selective electrode method described in GB 7484–87 (the national standard of the People's Republic of China, 1987) with the range of concentration from 0.05 to 1900 $mg \cdot dm^{-3}$. The calibration curve was plotted with fluoride concentrations from 1 to 10 $mg \cdot dm^{-3}$ versus potential (mV).

Adsorption experiments. Batch adsorption experiments were conducted to examine the effects of pH and coexistent anions as well as the adsorption isotherm and kinetics on the adsorption processes. The effects of pH, ranging from 3 to 9 using 0.1 $mol \cdot dm^{-3}$ NaOH or HCl solution on fluoride adsorption were examined for 10 $mg \cdot dm^{-3}$ fluoride solution. The effects of coexistent anions, such as CO_3^{2-}, PO_4^{3-}, Cl^-, SO_4^{2-}, and NO_3^- of the concentrations of 10–100 $mg \cdot dm^{-3}$, on the fluoride sorption were examined using 10 $mg \cdot dm^{-3}$ fluoride solution and pH of 5 maintained by 0.1 $mol \cdot dm^{-3}$ HCl or NaOH. The adsorption experiments were carried out for 12 h based on our previous studies, proving that the equilibration of fluoride adsorption could be reached after 6–12 h.

In the adsorption isotherm experiments, 0.1 g of BC was added to 50 cm^3 of fluoride solution of concentrations ranging from 2 to 20 $mg \cdot dm^{-3}$. The polypropylene flasks were shaken at 150 rpm for 12 h in a thermostatic shaker at 10, 25, 35 and 45 °C. Then the adsorbent was filtered with a 0.45 μm cellulose membrane filter. Equivalent volume of 10 cm^3 of filtrate and 10 cm^3 of buffer solution were rationed to 50 cm^3 volumetric flask, and the equilibrium fluoride concentration in the filtrate was measured using a fluoride meter equipped with a fluoride ion selective electrode.

For the adsorption kinetic experiments, 1.0 g of BC was respectively added to 1000 cm^3 fluoride solution of initial concentration of 5, 10 and 20 $mg \cdot dm^{-3}$. The agitation temperatures were maintained at 25 °C. The fluoride concentration of the solution was regularly analyzed during adsorption process.

The amount of fluoride ions adsorbed onto BC was calculated based on a difference of fluoride concentration between the initial and filtrate solution. All the adsorption experiments were repeatedly conducted with the errors of less than 5%. Thus, adsorption data were calculated by the average value of duplicate tests. The amount of adsorbed fluoride was calculated according to the equation:

$$q_e = \frac{V\left(C_0 - C_e\right)}{w} \text{ or } q_t = \frac{v\left(C_0 - C_t\right)}{w} \tag{1}$$

Regeneration and field trial. To understanding the onsite application of BC, a single cycle of adsorption-desorption was tested. Initially, 0.1 g of BC was added to 50 cm^3 of 10 $mg \cdot dm^{-3}$ fluoride solution for 12 h. pH of the solution was adjusted to 5 with 0.1 $mol \cdot dm^{-3}$ HCl or NaOH. The polypropylene flasks were shaken at 150 rpm for 12 h in a thermostatic shaker at 25 °C. Sequentially, the adsorbent was separated by filtration and washed with distilled water. The desorption of fluoride on BC and the regeneration of the adsorption media were conducted using NaOH solution ranging from 0.05 to 0.20 $mol \cdot dm^{-3}$, respectively. After the regeneration, the ability of BC adsorbent to remove fluoride from solution was again tested in an adsorption experiment using a similar procedure. The recycling regeneration experiment can be repeated in the same situation. The regeneration efficiency (η) was calculated from

$$\eta = \frac{q_n}{q_0} \times 100\% \tag{2}$$

In this study, the defluoridation applicability of BC was also demonstrated with the water sample taken from a nearby fluoride-endemic area. The parameters of water quality in the water sample, including pH, electrical conductivity and the concentration of F^-, Cl^-, Na^+, K^+ were analyzed. A sample solution of 50 cm^3 containing 0.1 g of BC in polypropylene flasks was shaken at 150 rpm in a thermostatic shaker at 25 °C for 12 h.

Determination of adsorbent properties. The surface morphology of the adsorbents was observed by using Scanning electro microscopy (SEM), (FEI Quanta 200, USA). Prior to the SEM observation, the whole samples were coated with Au on the surface to increase electric conductivity. Energy-dispersive X-ray spectroscopy (EDS), (InCA-Point&ID, England) was also used to analyze the element compositions on the adsorbent surface. XRD was carried out with a D/max-IIIV powder diffract meter using Cu-K_α radiation at a scanning range of 2θ of 10–80 deg with a speed of 6 deg·min^{-1} and a scan step of 0.02 deg. BC samples, before and after fluoride adsorption at the initial 10 mg·dm^{-3} blended with KBr were pressed into disks for FTIR analysis. Scans were repeatedly operated 32 times in the wavenumber range of 400–4000 cm^{-1}. The spectra were recorded on a FTIR spectrophotometer (Avatar FTIR 330, USA) under ambient conditions. TGA measurements were carried out on an SDT Q600 instrument (TA Instruments-Waters LLC, USA) in an N_2 atmosphere. The range of temperature was performed from 30 to 1000 °C with the gradient of 10 °C·min^{-1}. The surface area and pore size distributions of BC were determined from nitrogen adsorption at 77.15 K using an automatic Micromeritics Gemini VII Surface Area and Porosity. The Barrett–Joyner–Hanlenda (BJH) method was applied to calculate the pore size distribution. Prior to gas adsorption measurements, BC was degassed at 120 °C in a vacuum condition for 2 h. Nitrogen adsorption isotherms were measured under relative pressure (p/p_0) ranging from approximately 0.010 to 0.995.

pH_{pzc} was determined by the pH drift method. 50 cm^3 of 0.01 m·dm^{-3} NaCl solution was used in 100 cm^3 polypropylene flasks with the initial pH (pH_i) ranging from 3.0 to 10.0. Sequentially, 0.20 g of BC was added. These flasks were kept for 24 h in a thermostatic shaker at 25 °C. The equilibrium pH (pH_e) of the solution was measured and plotted against pH_i. pH at which the curve crossed $pH_i = pH_e$ line was taken as pH_{PZC} (Fig. 1a).

3. RESULTS AND DISCUSSIONS

3.1. PARAMETERS AFFECTING ADSORPTION OF FLUORIDE IONS ON BC

High adsorption ability at weak acid medium may be related to the surface charge of BC based on zero point of charge (pH_{pzc}), when the electrical charge density on a surface is zero [15]. The value of pH_{pzc} determined in this study (Fig. 1a) is 5.3, lower than 7.0–8.5 reported by other authors. It is located in the range of 4.35–7.8, similarly as pH_{pzc} of synthetic hydroxyapatite [16]. Apparently, the composition of BC may be a reason to explain the divergence of pH_{pzc} found in other references. If pH is below pH_{pzc}, more of the surface sites are positively charged and more fluoride ions could be adsorbed. If pH was above pH_{pzc}, the surface charge is negative; fluoride ions will be adsorbed to a lesser extent due to the repulsive forces between fluoride ions and negative charge [17].

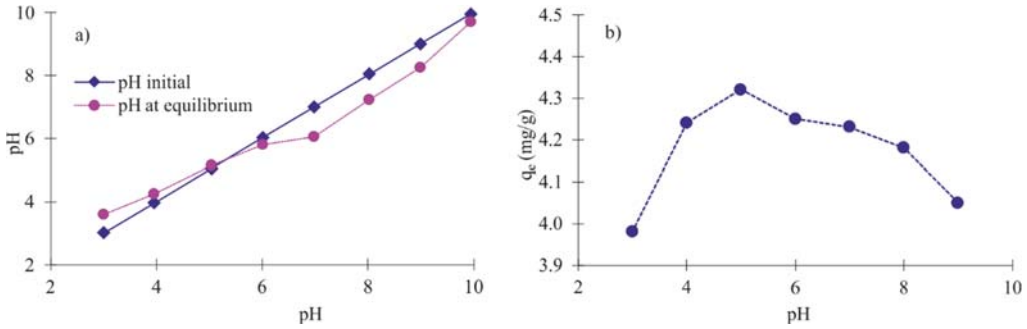

Fig. 1. pH at equilibrium against initial pH (a), fluoride adsorption capacities vs. pH (b)

At pH 3.0, the low adsorption capacity may be due to the fact that molecules of udissociated hydrofluoric acid, not fluoride anions prevail in the solution [18]. In addition, other possible reason was related with the ionization of hydroxyl group resulting in slight dissolution of BC at a strong acid medium. For pH < 5.3, the BC surface due to deprotonation of the hydroxyl groups acquires a negative charge, causing the decrease of adsorption for negatively charged fluoride ions.

The effect of pH within the range of 3.0–9.0 is presented in Fig. 1b. At low region of initial pH value, the amount of fluoride ions adsorbed at equilibrium (q_e) increased slightly upon increasing pH. In the range of pH 3.0–5.0, the equilibrium pH value (pH_e) changed from 3.6 to 5.15 corresponding to the increase of q_e from 3.96 $mg \cdot g^{-1}$ to maximum value of 4.27 $mg \cdot g^{-1}$. For pH higher than 5.0, q_e decreased upon increasing pH.

In natural water, several common anions, including chloride, sulfate, nitrate, phosphate and carbonate ions, exist simultaneously in different concentrations to compete with the removal of fluoride ions by adsorbents. In natural water, several common anions, including chloride, sulfate, nitrate, phosphate and carbonate ions, exist simultaneously in various concentrations, competing with the removal of fluoride ions by adsorbents. In Figure 2, the amounts of fluoride ions (q_e) adsorbed onto BC in the presence of other ions are shown. It is visible that different ions at various concentrations possessed different effects on q_e. The amount of fluoride ions adsorbed on BC increases with increasing amount of chloride and nitrate ions, probably due to the increase in the ionic strength of the solution or the weakness of the lateral repulsion between adsorbed fluoride ions at pH 5.0 [19].

An opposite effect was observed for sulfate and carbonate ions, whose presence diminished q_e. A possible explanation is that this resulted from the competition of both ions with fluoride on adsorption sites owing easier adsorption multivalent anions than monovalent ones. However, the increase of Culombic repulsive forces reducing probability of fluoride interacting with the active sites could also play important role [20]. Phosphate ions do not affect fluoride sorption onto BC. In the crystal structure of apatite, F^- ions can be substituted for OH^- ions in BC, yielding more thermodynamically stable

fluorapatite ($Ca_{10}(PO_4)_6F_2$). In contrast to fluoride ion, phosphate ion appears to be larger than fluoride ion, thus it can be easily accommodated [21].

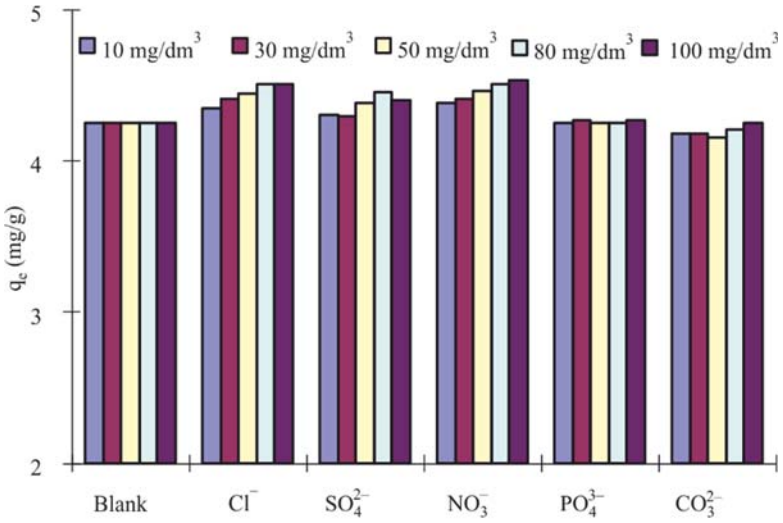

Fig. 2. Effects of coexisting anions on fluoride adsorption on BC

3.2. CHARACTERIZATION OF BC BEFORE AND AFTER FLUORIDE ADSORPTION

The surface morphology and element composition were examined by SEM-EDS. The morphology of BC particles shown in Fig. 3a reveals the presence of fractured and porous surface on irregular particles. The EDS analysis (Fig. 3b) indicates that the dominant elements such as Ca, P and O are present on the surface of BC, and their relative percentages are 35.22, 16.92, and 47.86 wt. %, respectively.

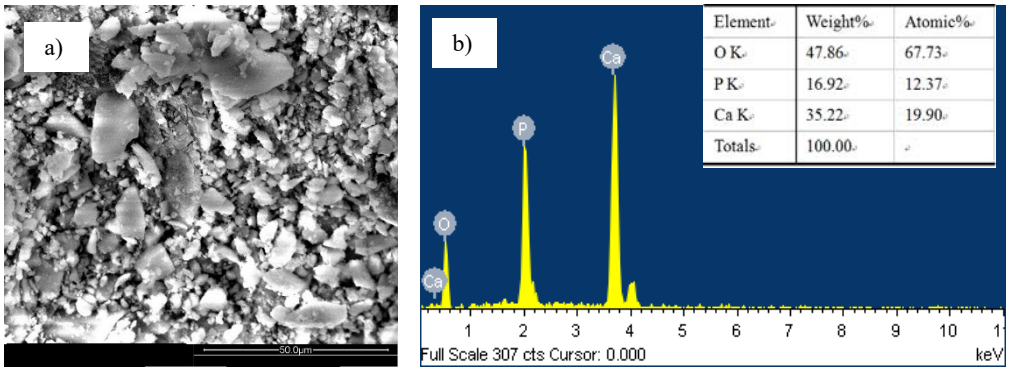

Fig. 3. SEM image (a), and EDS result (b) for BC

BC is a composite material of $Ca_5(PO_4)_3OH$ and $Ca_3(PO_4)_2 \cdot xH_2O$. The XRD patterns and FTIR spectra of BC with and without fluoride adsorbed are shown in Figs. 4, 5, respectively. The XRD of BC without fluorides had four main peaks located at 2θ of 25.9°, 28.0°, 32.0°, and 40.0°. There is no marked change in the XRD pattern of BC after adsorption (Fig. 4). Only F^- ions have been replaced with hydroxyl functional groups of bone char. This finding is similar to the report of Poinerna [22] on the fluoride adsorption onto hydroxyapatite.

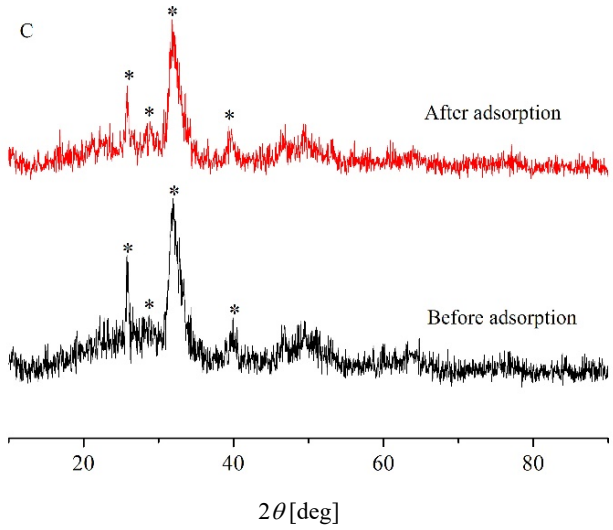

Fig. 4. XRD patterns of BC

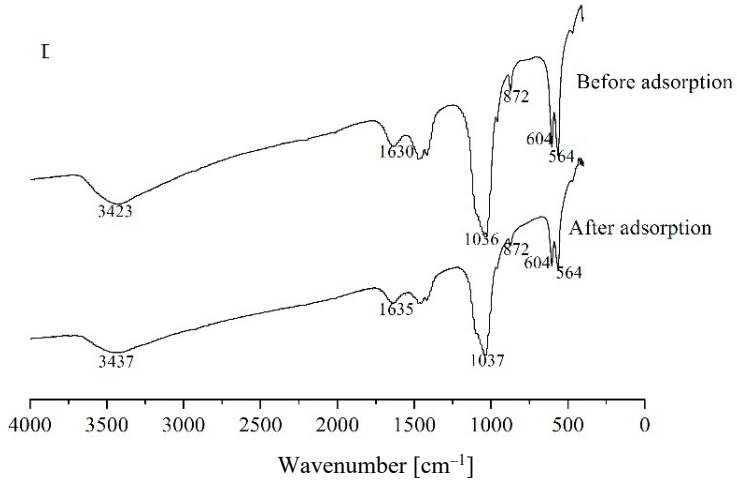

Fig. 5. FTIR spectra of BC

FTIR spectra of BC before and after fluoride adsorption are presented in Fig. 5. The bands at ca. 3423 and 1630 cm^{-1} may be attributed to the characteristic stretching and the bending vibrations of the hydroxyl group, respectively. Typical apatite phosphate modes appearing at 1036, 604 and 564 cm^{-1} were assigned to the formation of pure apatite [23]. After adsorption, the bands at 3423 and 1630 cm^{-1} were shifted to 3437 and 1635 cm^{-1}, respectively, demonstrating the phenomenon of the interchangeability between fluoride in bulk solution and hydroxyl groups on BC sorbent.

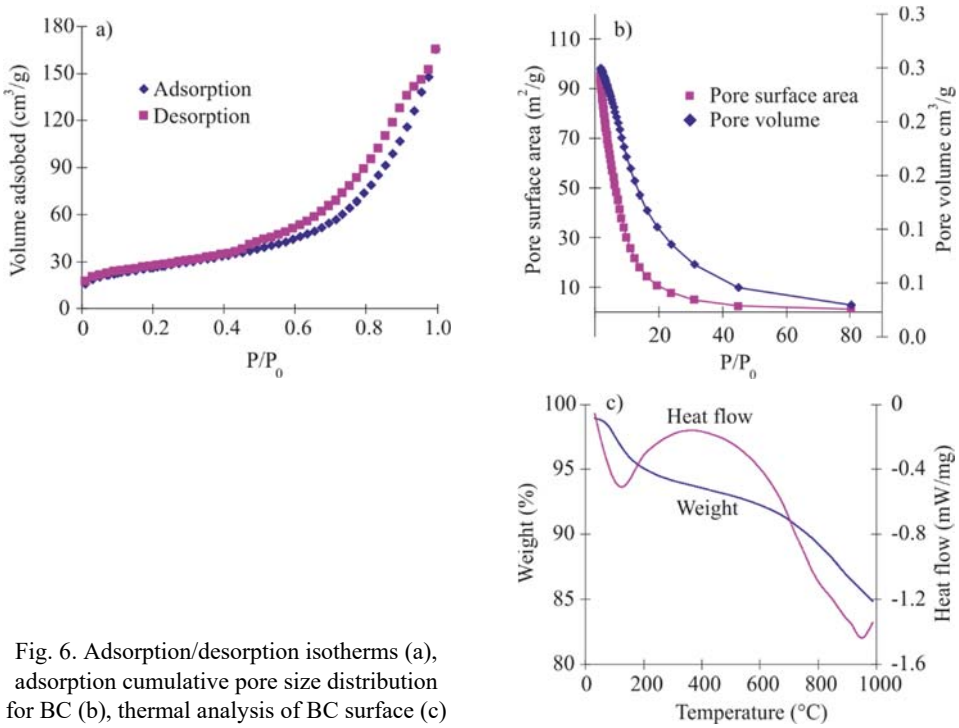

Fig. 6. Adsorption/desorption isotherms (a), adsorption cumulative pore size distribution for BC (b), thermal analysis of BC surface (c)

Figure 6a shows the isotherms of adsorption/desorption for the BC material. The adsorbed volume increased upon increasing P/P_0, indicating a wide pore size distribution in BC. The adsorption isotherm of BC could be classified to type IV because of typical mesoporous nature of the material [24]. The steep gradient in Fig. 6a may be related with limitation to the uptake of nitrogen owing to capillary condensation in the mesopores. Based on the pore size distribution closely related to both kinetic and equilibrium properties of the porous material, this implies that the structural heterogeneity of porous materials potentially has its application in industry [22].

BC has a wide pore size distribution, as shown in Fig. 6b. The BET surface area of BC was 92.33 $m^2 \cdot g^{-1}$, whereas the BJH adsorption/desorption surface area of pores was 95.36/111.06 $m^2 \cdot g^{-1}$. The single point of the total pore volume was found to be

0.2556 $cm^3 \cdot g^{-1}$, whereas BJH adsorption/desorption cumulative volume of pores (1.70 nm < d < 300 nm) was 0.2501/0.2549 $cm^3 \cdot g^{-1}$, respectively. Pore sizes of BC were classified as micropores (d < 2 nm), mesopores (2 nm < d < 50 nm) and macropores (d > 50 nm). According to BJH adsorption cumulative distribution of pore size in BC, the percentages of micro- meso- and macropores were 3.59%, 88.54% and 1.31%, respectively, indicating that mesopores dominated in the surface structure of BC.

As shown in Figure 6c, three stages of thermal decomposition of BC were observed from its TGA. The weight loss was close to 14% from 30 °C to 1000 °C. First endothermic stage with the weight loss of 3.92% up to 200 °C may be related to the loss of moisture. The heat flow analysis in Fig. 6c shows a broad endothermic peak at ca. 120 °C which corresponded to a great amount of water loss upon heating. Second endothermic stage from 200 °C to 700 °C, indicated a major loss of chemisorbed water. These effects were also observed by Younesi [25]. Finally, a weight loss of 6.22% was observed between 700 °C and 1000 °C attributed to the partial dehydroxylation process and decomposition of BC. The phenomena of hydroxyl ion escape from BC might be due to dehydroxylation process during thermal treatment. The final weight loss at 950 °C was mainly due to by thermal decomposition of BC [25] .

3.3. ADSORPTION ISOTHERMS

Several applicable isotherm models are widely used, such as the Langmuir and the Freundlich models. The Freundlich model is a purely empirical one. The Langmuir model assumes however, the occurrence of the maximum adsorption when the surface has been covered by a single layer of adsorbate. The Langmuir isotherm can be expressed as [22]:

$$q_e = \frac{QbC_e}{1 + bC_e} \tag{3}$$

The Freundlich isotherm equation is given by

$$q_e = K_F C_e^{1/n} \tag{4}$$

n > 1 indicates a favorable situation for adsorption.

Figure 7a shows the adsorption isotherms of the removal of fluoride ions onto BC at 10, 25, 35, and 45 °C, respectively. The plots of equilibrium amount of fluoride ions uptake (q_e) against the equilibrium concentration (C_e) in the solution indicate that the equilibrium concentration of fluoride ions on BC gradually increased upon decreasing fluoride concentration in the bulk solution. The higher temperature, the more prononuced change occurred. The q_e value gradually increased upon increasing temperature

from 10 °C to 45 °C, possibly indicating that the interaction between fluoride ions and BC is an endothermic reaction in nature. A positive value of $\Delta H°$ also indicates an endothermic nature of the adsorption process [4].

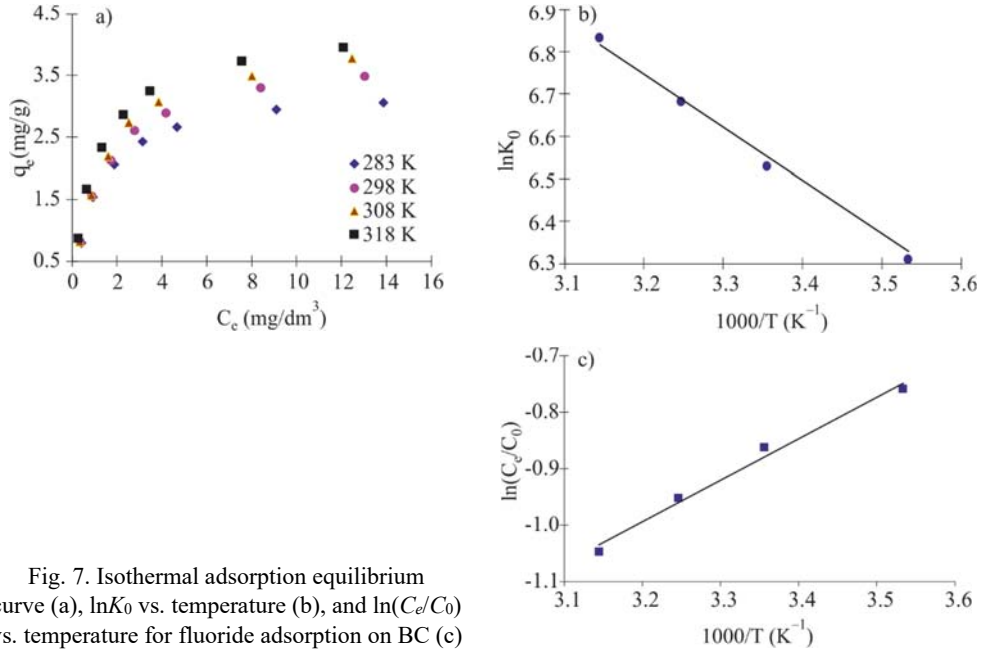

Fig. 7. Isothermal adsorption equilibrium curve (a), lnK_0 vs. temperature (b), and ln(C_e/C_0) vs. temperature for fluoride adsorption on BC (c)

Table 1

Parameters of the Langmuir and Freundlich models

Temperature [K]	Langmuir				Freundlich			
	Q [mg·g^{-1}]	b	R^2	χ^2	K_F [mg$^{(1-1/n)}$·mol$^{1/n}$·g^{-1}]	n	R^2	χ^2
283	3.335	0.840	0.9972	0.00187	1.576	3.546	0.8842	0.07760
298	3.852	0.714	0.9988	0.00111	1.676	3.195	0.9060	0.08764
308	4.185	0.697	0.9983	0.00162	1.782	3.096	0.9081	0.10371
318	4.280	0.900	0.9992	0.00095	2.000	3.311	0.9115	0.11071

The adsorption data were fitted with the Langmuir and Freundlich models. The equilibrium parameters are listed in Table 1. The higher correlation ($R^2 > 0.99$) in the Langmuir than the Freundlich models ($R^2 < 0.92$) indicates that the Langmuir isotherm was superior to the Freundlich isotherm for the fluoride ions adsorption on BC. The $\chi 2$ value could also support the fitness of the model. The $\chi 2$ values for the Langmuir iso-

therm were lower, indicating that the Langmuir isotherm was more suitable for the sorption of fluoride on BC. A similar report was found in the study of the fluoride adsorption onto selective ion-exchange resin [26].

In order to find out the feasibility of the isotherm, the essential characteristics of the Langmuir isotherm can be expressed in terms of a dimensionless quantity *r*:

$$r = \frac{1}{1 + bC_0} \tag{5}$$

Table 2

Dimensionless factor (*r)* values of the Langmuir isotherm at various initial concentrations

Temperature [K]	C_0 [mg·dm^{-3}]						
	2	4	6	8	10	15	20
283	0.373	0.229	0.166	0.130	0.106	0.074	0.056
298	0.412	0.259	0.189	0.149	0.123	0.085	0.065
308	0.418	0.264	0.193	0.152	0.125	0.087	0.067
318	0.357	0.217	0.156	0.122	0.100	0.069	0.053

The calculated constants are summarized in Table 2. The *r* values for the adsorption of fluoride on BC were located in the range of 0.053–0.418, indicating that the shape of the isotherm is favourable [14].

3.4. ADSORPTION THERMODYNAMICS

The fluoride adsorption onto BC was endothermic in nature similar to those reported in the literature [41, 17]. In order to test the feasibility and spontaneity of the adsorption process, the thermodynamic parameters of free energy change ($\Delta G°$), enthalpy change ($\Delta H°$) and entropy change ($\Delta S°$) were calculated at each temperature according to the following equation:

$$\Delta G° = -RT \ln K_D \tag{6}$$

The van't Hoff equation is expressed as

$$\ln K_D = \frac{\Delta S°}{R} - \frac{\Delta H°}{RT} \tag{7}$$

where K_D can be calculated from:

$$K_D = \frac{q_e}{C_e} \tag{8}$$

Because both $\Delta G°$ and the term of RT have the unit of $J \cdot mol^{-1}$, the equilibrium constant K_D in Eq. (6) should be dimensionless. In order to make K_D be dimensionless, the method suggested by Poinerna et al. [22] was adopted in this research. Thus, the equilibrium constant K_D in Eq. (6) should be replaced by a new dimensionless equilibrium constant, namely K_0.

$$K_0 = \frac{\rho q_e}{C_e} \tag{9}$$

The van't Hoff equation was used to calculate the change in entropy, $\Delta S°$, and the change in enthalpy, $\Delta H°$ for the process of adsorption. From the intercept and slope of $\ln K_0$ vs. $1/T$ (Fig. 7b) $\Delta S°$ and $\Delta H°$ were determined to be 89.443 $J \cdot mol^{-1} \cdot K^{-1}$, and 10.426 $kJ \cdot mol^{-1}$, respectively. A positive value of $\Delta H°$ indicates an endothermic nature of the adsorption process. $\Delta S°$ with positive value is associated with an increase in randomness on the BC surface.

Table 3

Thermodynamic parameters for defluoridation by BC

Temperature [K]	$\Delta G°$ [$kJ \cdot mol^{-1}$]	$\Delta H°$ [$kJ \cdot mol^{-1}$]	$\Delta S°$ [$J \cdot mol^{-1} \cdot K^{-1}$]	E_a [$kJ \cdot mol^{-1}$]	S^*
283	–14.923	10.426	89.443	6.136	0.0348
298	–16.175				
308	–17.108				
318	–18.061				

As listed in Table 3, in the examined range of temperatures $\Delta G°$ values are negative, proving not only the feasibility and spontaneity of the adsorption process in nature. The decrease in $\Delta G°$ upon increasing temperature shows that the adsorption of fluoride ions on BC is more spontaneous at high temperatures. Usually, for physical adsorption $\Delta G°$ ranges from –20 to 0 $kJ \cdot mol^{-1}$ and for chemical adsorption from –80 to –400 $kJ \cdot mol^{-1}$ [36]. The values obtained in this study point to physical adsorption of fluoride ions on BC material.

3.5. ACTIVATION ENERGY OF FLUORIDE ADSORPTION ONTO BC

To further demonstrate the fact that physical adsorption is the key reaction, the values of activation energy (E_a) and the surface coverage (θ) were computed using the Arrhenius equation based on the experimental data:

$$\ln k = \ln A - \frac{E_a}{RT} \tag{10}$$

$$\theta = 1 - \frac{C_e}{C_0} \tag{11}$$

$$\ln\left(1-\theta\right) = \ln S^* + \frac{E_a}{RT} \tag{12}$$

where S^* is the sticking probability, which is a function of the adsorbate/adsorbent system. The value of fluoride ions adsorption onto BC conducted was 0.0348 ranging from 0 to 1, indicating that the adsorption process was a physical adsorption [43]. The activation energy was calculated as 6.136 kJ·mol^{-1} from the slope of $\ln(C_e/C_0)$ vs. $1/T$ (Fig. 7c), showing that its value was characteristic of physical adsorption (5–40 kJ·mol^{-1}), much lower than of chemical adsorption (40–800 kJ·mol^{-1}) [27].

3.6. ADSORPTION KINETICS

Successful application of the adsorption technique must possess a vivid advantage including available recycled adsorbents, known kinetic parameters, and adsorption characteristics. Therefore the kinetic analysis is essential for any adsorption study. Several kinetic models have been applied to test the fitness of the experimental data obtained in this research [28].

The pseudo-first order equation can be expressed as

$$\ln\left(q_e - q_t\right) = \ln q_e - k_1 t \tag{13}$$

The pseudo-second order equation for sorption kinetics is:

$$\frac{t}{q_t} = \frac{1}{k_2 q_e^2} + \frac{t}{q_e} \tag{14}$$

The intraparticle diffusion model for sorption kinetics can be formulated as

$$q_t = k_p t^{1/2} + C \tag{15}$$

The plots of the three kinetic models are shown in Fig. 8. The values of kinetic parameters from the fitting results are summarized in Table 4. The kinetics data of fluoride adsorption onto BC could be successfully simulated by the pseudo-second order equation with a higher correlation coefficient (0.9965–0.9986) than for the others (0.9035–0.9822). In addition, the equilibrium adsorption capacity calculated from the second-order model is in agreement with the experimental value.

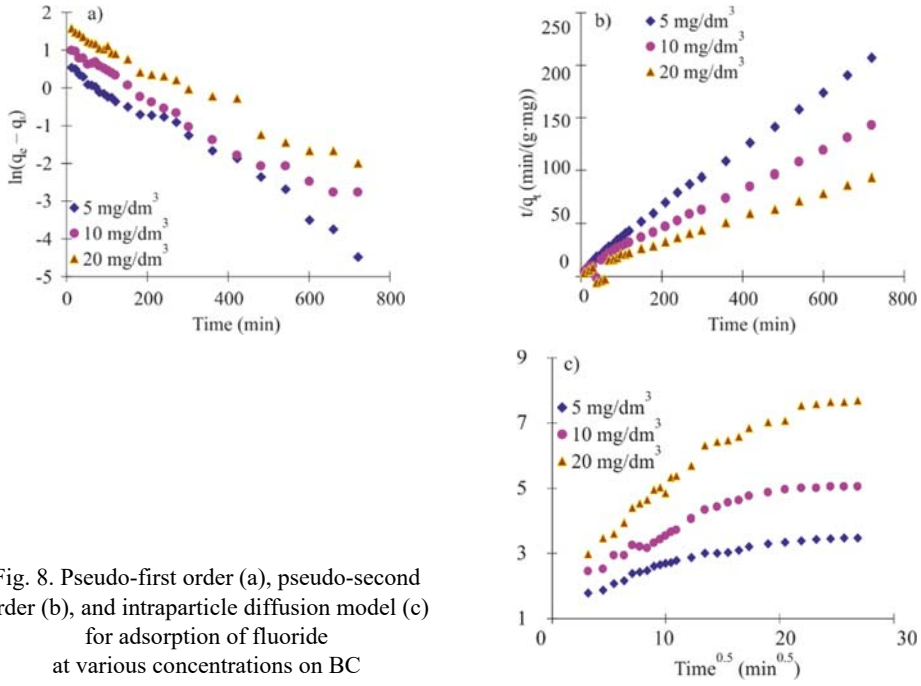

Fig. 8. Pseudo-first order (a), pseudo-second order (b), and intraparticle diffusion model (c) for adsorption of fluoride at various concentrations on BC

Table 4

Fitted parameters and SSE values of adsorption kinetic models

Model	Parameter	C_0 [mg·dm^{-3}]		
		5	10	20
Pseudo-first order	R^2	0.9849	0.9822	0.9849
	$q_{e,cal}$, mg·g^{-1}	1.6970	2.5670	4.5660
	k_1, min^{-1}	0.0064	0.0058	0.0051
	SSE	0.2639	0.2467	0.1742
Pseudo-second order	R^2	0.9986	0.9979	0.9965
	$q_{e,cal}$, mg·g^{-1}	3.5958	5.3277	8.1500
	k_2, g·min^{-1}·mg^{-1}	0.0091	0.0049	0.0024
	SSE	0.0009	0.0020	0.0018
Intra-particle diffusion	R^2	0.9035	0.9150	0.9386
	k_P, mg·min$^{-1/2}$·mg^{-1}	0.0696	0.1188	0.2018
	C	0.8721	2.3570	2.9679
	SSE	0.0004	0.1120	0.1287

Intraparticle diffusion may be the rate-limiting step. It seems that every curve in Fig. 8c consists of three parts being straight lines. Starting from left, the first line, corresponds to the external diffusion of adsorbate through the boundary layer to the surface

of adsorbent. The second line, with a smaller slope, describes the gradual adsorption, dominant by the intraparticle diffusion process. The latter one represents the equilibrium stage of the chemical reaction, when the diffusion process begins to slow down owing to low solute concentration [7].

The assessment of the kinetic models employed for fitting the sorption data was calculated by the sum of errors squared (SSE). Low values of SSE not only show a better fit to adsorption data but also demonstrate that the pseudo-second order provides much better fitting to the experimental data than the other two models.

$$\mathrm{SSE} = \sum \frac{\left(q_{t,\mathrm{exp}} - q_{t,\mathrm{cal}}\right)^2}{q_{t,\mathrm{exp}}^2} \tag{16}$$

3.7. REGENERATION EXPERIMENTS AND FIELD TEST

The convenient regeneration of exhausted adsorbent was regarded as a crucial factor if adsorption processes could be applied into field operation. In this study, NaOH of various concentrations was used as a solution for regeneration. Regeneration efficiency vs. concentration of sodium hydroxide is shown in Fig. 9a, indicating that for 0.2 mol·dm^{-3} NaOH, the efficiency of 91.2% could be reached. In other words, the ion-exchange of hydroxyl groups with fluoride ions on BC adsorbents is efficient in strong alkaline solution. In order to check the repeatability of BC, successive adsorption-desorption cycles were conducted. As shown in Fig. 9b, a considerable reduction in adsorption efficiency occurred in the second and third cycle of adsorption after the regeneration. At the end of the third cycle, 85% regeneration efficiency was observed, revealing that BC had the following advantages including the operation with recycling, the effective facility with reasonable cost and the possible application into field.

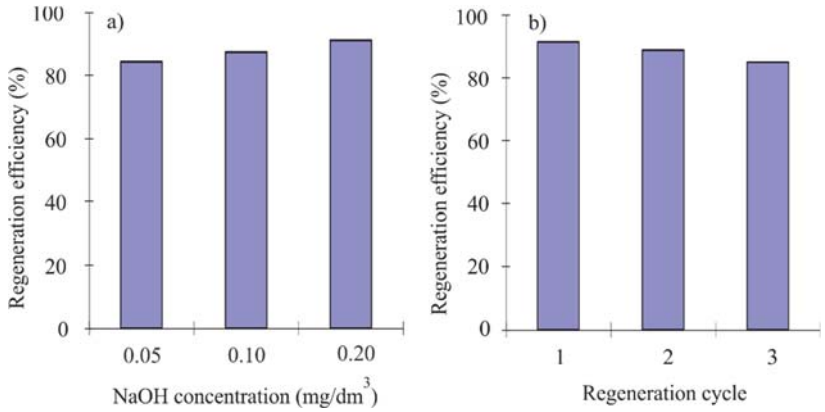

Fig. 9. Regeneration efficiencies at various sodium hydroxide concentrations (a), and cycles for original BC with fluoride adsorption (b)

The defluoridation efficiency of BC conducted with a water sample from field level was also completed in this research (Table 5). Concentration of fluoride ions decreased from 6.2 mg·dm^{-3} to 0.61 mg·dm^{-3}. Electrical conductivity was kept constant after application of BC, indicating the minute variation of concentrations of Cl^-, Na^+ and K^+ ions.

Table 5

Field trial results for bone char

Water quality parameter	Before treatment	After treatment
F^-, mg·dm^{-3}	6.20	0.61
pH	3.12	5. 40
Electrical conductivity, mS·cm^{-1}	0.72	0.70
Cl^-, mg·dm^{-3}	55.00	50.00
Na^+, mg·dm^{-3}	40.00	38.50
K^+, mg·dm^{-3}	10.10	10.00

The concentration of fluoride ions in the treated water is well within the tolerance limit of regulation in China. Briefly, fluoride removal onto BC was controlled by both adsorption and ion exchange. The possible reactions routes are as follows:

- adsorption:

$$Ca_{10}(PO_4)_6(OH)_2 + Ca^{2+} + 2F^- \rightarrow Ca_{10}(PO_4)_6(OH)_2 \cdot CaF_2$$

- ion exchange:

$$Ca_{10}(PO_4)_6(OH)_2 + nF^- \rightarrow Ca_{10}(PO_4)_6(OH)_{2-n}F_n + nOH^-$$

- regeneration desorption mechanism:

$$Ca_{10}(PO_4)_6(F)_2 \cdot CaF_2 + 4OH^- \rightleftarrows Ca_{10}(PO_4)_6(OH)_2 \cdot Ca(OH)_2 + 4F^-$$

4. CONCLUSIONS

The basic properties of bone char include wide pore size distribution (0–50 nm) with BET surface area of 92.33 m^2·g^{-1}, and BJH adsorption/desorption surface area of 95.36/111.06 m^2·g^{-1}. The zero point pH of BC was located at acidic range (pH = 5.3) having a maximum fluoride ions removal rate, the adsorption capacity was 4.45 mg/g. Several anions, including Cl^-, SO_4^{2-}, NO_3^-, PO_4^{3-}, and CO_3^{2-} at various concentrations had different effects on the fluoride sorption. When multivalent anions were co-present, the BC had better adsorption efficiency, and the adsorption order followed as $Cl^- > NO_3^-$

> SO_4^{2-} > PO_4^{3-} > CO_3^{2-}. The morphology and composition of BC reveals the presence of a fractured and porous surface in the irregular particles having dominant elements of Ca, P and O. Subtle change in the XRD pattern of BC after fluoride adsorption was observed with respect to original BC; however, the interchangeability between fluoride in bulk solution and hydroxyl groups on BC sorbent was proved by FTIR. Fluoride ion adsorption isotherms on BC were well fitted using the Langmuir model. The thermodynamic parameters of fluoride adsorption process reveal the physical process, spontaneous reaction, endothermic and increasing randomness at the solid/solution interface.

The adsorption kinetic mechanism could be described by pseudo-second order model, however, pseudo-first order as well as the intraparticle diffusion model play an important role. Intraparticle diffusion may be the controlling step in fluoride ion removal by BC. The external mass transport is quite fast and does not control the overall rate of fluoride adsorption. Regeneration experiments demonstrated that fluoride absorbed on BC could be easily desorbed with sodium hydroxide solution, providing an available solution of the problem of excessive ingestion of fluoride in rural areas, especially in China.

ACKNOWLEDGMENTS

This project was supported by the National Science Foundation for Young Scholars of China (Grant No. 51406141 and 21407118) which belongs to the Project of Fujian Province Education Department (JA11262), and provides the Scientific and Technological Planning Project of Nanping (N2012Z06). The authors appreciate the help of the staff working in Wuyi University and Tajen University, especially for the students who conducted this experiment.

SYMBOLS

C_0 – initial fluoride concentration, $mg \cdot dm^{-3}$
C_e – equilibrium fluoride concentration, $mg \cdot dm^{-3}$
q_e – amount of fluoride adsorbed at equilibrium, $mg \cdot g^{-1}$
q_t – amount of fluoride adsorbed after time t, $mg \cdot g^{-1}$
C – fluoride concentration at time t, $mg \cdot dm^{-3}$
V – solution volume, dm^{-3}
w – amount of adsorbent, g
Q – Langmuir isotherm constant related to the capacity, $mg \cdot g^{-1}$
b – Langmuir adsorption equilibrium constant, $dm^3 \cdot mg^{-1}$.
K_F – empirical constant of Freundlish isotherm, $mg^{(1-1/n)} \cdot mol^{1/n} \cdot g^{-1}$
n – empirical constants of Freundlish isotherm
K_D – thermodynamic equilibrium constant, $dm^3 \cdot g^{-1}$
ρ – density of water, $g \cdot dm^{-3}$
$\Delta G°$ – free energy change, $kJ \cdot mol^{-1}$
$\Delta H°$ – enthalpy change, $kJ \cdot mol^{-1}$
$\Delta S°$ – entropy change, $J \cdot mol^{-1} \cdot K^{-1}$
R – molar gas constant, $J \cdot mol^{-1} \cdot K^{-1}$

T – temperature, K
E_a – activation energy, $kJ \cdot mol^{-1}$
S^* – sticking probability
θ – surface coverage
k_1 – pseudo-first order adsorption rate constant, min^{-1}
k_2 – pseudo-second order adsorption rate constant, $g \cdot min^{-1} \cdot mg^{-1}$
k_p – intraparticle diffusion rate constant, $mg \cdot min^{-1/2} \cdot g^{-1}$
C – intercept providing an idea of the boundary layer thickness
$q_{e,\,exp}$ – experimental adsorption capacity data, $mg \cdot g^{-1}$
$q_{e,\,cal}$ – theoretical adsorption capacity data, $mg \cdot g^{-1}$

REFERENCES

[1] MAITI A., BASU J.K., DE S., *Chemical treated laterite as promisingfluoride adsorbent for aqueous system and kinetic modeling*, Desalin., 2011, 265, 28.

[2] KAMBLE S.P., *Defluoridation of drinking water using chemically modified bentonite clay*, Desalin., 2009, 249, 687.

[3] MOURABET M., RHILASSI A.E., BENNANI-ZIATNI M., EL HAMRI R., TAITAI A., *Studies on fluoride adsorption by apatitic tricalcium phosphate (ATCP) from aqueous solution*, Desalin. Water Treat., 2013, 51, 34.

[4] LIU H., DENG S.B., LI Z.J., YU G., HUANG J., *Preparation of Al-Ce hybrid adsorbent and its application for defluoridation of drinking water*, J. Hazard. Mater., 2010, 179, 424.

[5] ZHANG T., LI Q., XIAO H., MEI Z., LU H., ZHOU Y., *Enhanced fluoride removal from water by non-thermal plasma modified CeO_2/Mg–Fe layered double hydroxides*, Appl. Clay Sci., 2013, 72, 117.

[6] CHEN H., YAN M., YANG X., CHEN Z., WANG G., SCHMIDT-VOGT D., XU Y., XU J., *Spatial distribution and temporal variation of high fluoride contents in groundwater and prevalence of fluorosis in humans in Yuanmou County, Southwest China*, J. Hazard. Mater., 2012, 235–236, 201.

[7] LV L., HE J., WEI M., EVANS D.G., ZHOU Z.L., *Treatment of high fluoride concentration water by MgAl-CO_3 layered double hydroxides. Kinetic and equilibrium studies*, Water Res., 2007, 41, 1534.

[8] LOGANANATHAN P., VIGNESWARAN S., KANDASAMY J., NAIDU R., *Defluoridation of drinking water using adsorption processes*, J. Hazard. Mater., 2013, 248–249, 1.

[9] GAO S., CUI J., WEI Z., *Study on the fluoride adsorption of various apatite materials in aqueous solution*, J. Fluor. Chem., 2009, 130 (11), 1035.

[10] SMICIKLAS I., DIMOVIC S., SLJIVIC M., PLECAS I., *The batch study of Sr^{2+} sorption by bone char*, J. Environ. Sci. Health A, 2008, 43 (2), 210.

[11] CHEUNG C.W., CHAN C.K., PORTER J., MCKAY F.G., *Combined Diffusion Model for the Sorption of Cadmium, Copper, and Zinc Ions onto Bone Char*, Environ. Sci. Technol., 2001, 35 (7), 1511.

[12] KO D.C.K., CHEUNG C.W., CHOY K.K.H., PORTER J.F., MCKAY G., *Sorption equilibria of metal ions on bone char*, Chemosphere, 2004, 54 (3), 273.

[13] CHEUNG C.W., PORTER J.F., MCKAY G., *Sorption kinetic analysis for the removal of cadmium ions from effluents using bone char*, Water Res., 2001, 35 (3), 605.

[14] MEDELLIN-CASTILLO N.A., LEYVA-RAMOS R., OCAMPO-PEREZ R., GARCIA R.F., ARAGON-PIRIA A., MARTINEZ-ROSALES J.M., GUERRERO-CORONADO R., FUENTES-RUBIO M.L., *Adsorption of fluoride from water solution on bone char*, Ind. Eng. Chem. Res., 2007, 46 (26), 9205.

[15] MA Y., SHI F., ZHENG X., MA J., GAO C., *Removal of fluoride from aqueous solution using granular acid-treated bentonite (GHB). Batch and column studies*, J. Hazard. Mater., 2011, 185 (2–3), 1073.

[16] GAO S., SUN R., WEI Z.G., ZHAO H., LI H., HU F., *Size-dependent defluoridation properties of synthetic hydroxyapatite*, J. Fluor. Chem., 2009, 130, 550.

[17] TOR A., DANAOGLU N., ARSLAN G., CENGELOGLU Y., *Removal of fluoride from water by using granular red mud. Batch and column studies*, J. Hazard. Mater., 2009, 164 (1), 271.
[18] KAMBLE S.P., DESHPANDE G., BARVE P.P., RAYALU S., LABHSETWAR N.K., MALYSHEW A., KULKAMI B.D., *Adsorption of fluoride from aqueous solution by alumina of alkoxide nature. Batch and continuous operation*, Desalin., 2010, 264 (1–2), 15.
[19] ONYANGO M.S., KOJIMA Y., KUMAR A., KUCHAR D., KUBOTA M., MATSUDA H., *Uptake of fluoride by Al^{3+} pretreated low-silica synthetic zeolites: adsorption equilibrium and rate studies*, Sep. Sci. Technol., 2006, 41 (4), 683.
[20] ESKANDARPOUR A., ONYANGO M.S., OCHIENG A., ASAI S., *Removal of fluoride ions from aqueous solution at low pH using schwertmannite*, J. Hazard. Mater., 2008, 152 (2), 571.
[21] AOBA T., *The effect of fluoride on apatite structure and growth*, Crit. Rev. Oral Biol. Med., 1997, 8 (2), 136.
[22] POINERNA G.E.J., GHOSH M.K., NG Y.J., ISSA T.B., ANAND S., SINGH P., *Defluoridation behavior of nanostructured hydroxyapatite synthesized through an ultrasonic and microwave combined technique*, J. Hazard. Mater., 2011, 185 (1), 29.
[23] ROJAS-MAYORGA C.K., BONILLA-PETRICIOLET A., AGUAYO-VILLARREAL I.A., HERNANDEZ-MONTOYA V., MORENO-VIRGEN M.R., MONTES-MORAN M.A., *Optimization of pyrolysis conditions and adsorption properties of bone char for fluoride removal from water*, J. Anal. Appl. Pyrol., 2013, 104, 10.
[24] WANG G., LIU H., LIU J., QIAO S., LU G.M., MUNROE P., AHN H., *Mesoporous $LiFePO_4$/C Nanocomposite Cathode Materials for High Power Lithium Ion Batteries with Superior Performance*, Adv. Mater., 2010, 22 (44), 4944.
[25] YOUNESI M., JAVADPOUR S., BAHROLOLOOM M.E., *Effect of heat treatment temperature on chemical compositions of extracted hydroxyapatite from bovine bone ash*, J. Mater. Eng. Perform., 2011, 20 (8), 1484.
[26] MEENAKSHI S., VISWANATHAN N., *Identification of selective ion-exchange resin for fluoride sorption*, J. Coll. Interf. Sci., 2007, 308 (2), 438.
[27] NOLLET H., ROELS M., LUTGEN P., VANDER M.P., VERSTRAETE W., *Removal of PCBs from wastewater using fly ash*, Chemosphere, 2003, 53 (6), 655.
[28] MANDAL S., MAYADEVI S., *Defluoridation of water using as-synthesized Zn/Al/Cl anionic clay adsorbent: Equilibrium and regeneration studies*, J. Hazard. Mater., 2009, 167 (1–3), 873.